Stag3D: A code for modeling thermo-chemical multiphase convection in Earth's mantle

P.J. Tackley[a,b], S. Xie[a]
[a]*UCLA Department of Earth and Space Sciences, Los Angeles, CA90095, USA*
[b]*UCLA Institute of Geophysics and Planetary Physics, Los Angeles, CA90095, USA*

Abstract
Realistic modeling of convection in Earth's mantle requires treatment of strong viscosity variations, solid-solid phase changes, and compositional differentiation. Here the implementation of these features into a 3-D finite volume code is discussed, and sample results presented. The resulting model appears very promising for studying Earth's thermochemical evolution.

Keywords: Mantle convection; infinite Prandtl number; Multigrid; Multiphase.

1. Introduction

Modeling convection in Earth's 2900 km deep mantle is challenging due to the multi-rheological and multi-compositional nature of mantle materials (e.g., Schubert, et al. [1]). For studying long-term evolution, viscous creep is the most important deformation mechanism, but viscosity is strongly dependent on temperature, pressure and often strain rate, varying by many orders of magnitude over ~100 km thick boundary layers and convective upwelling and downwellings. Partial melting at shallow (< 80km) depth and resulting crustal formation causes the system to progressively differentiate in compositionally, while convective stirring acts to rehomogenize the system. The nondiffusive nature of compositional variations presents a modeling challenge. The rocks that constitute the mantle are multi-mineralogical and undergo a series of solid-solid phase transitions with increasing pressure, the details of which depend on bulk composition. These are important dynamically because these cause lateral density variations that influence convection.

Here a code that can treat many of the above complexities is presented. Previous developments are summarized then the implementation of two processes is focused on: melting and differentiation, and multi-mineralogical phase transitions.

2. Physical model

The infinite Prandtl number and compressible anelastic approximations are assumed, leading to the following nondimensional (to thermal diffusion scales) equations for conservation of mass:

$$\nabla \cdot (\rho \underline{v}) = 0 \tag{1}$$

momentum

$$\nabla \cdot \left[\eta (v_{i,j} + v_{j,i} - \tfrac{2}{3} v_{k,k} \delta_{ij}) \right] - \nabla p = Ra.\ \hat{\underline{z}}.\rho(C,z,T) / \rho_{thermal} \tag{2}$$

energy

$$\rho C_p \frac{DT}{Dt} = Di_s \rho T v_z + \nabla \cdot (\bar{k} \nabla T) + \rho H + \frac{Di_s}{Ra} \tau_{ij} (v_{i,j} + v_{j,i} - \tfrac{2}{3} v_{k,k} \delta_{ij}) v_{i,j} \tag{3}$$

and bulk chemistry

$$\frac{\partial C}{\partial t} = -\underline{v} \cdot \nabla C . \quad (4)$$

The variables are temperature T, composition C, velocity $\underline{v}$ and pressure p. The governing parameters are Rayleigh number Ra, internal heating rate H, and surface dissipation number Di_s. Material properties with overbars (density $\bar{\rho}$, thermal expansivity $\bar{\alpha}$, and thermal conductivity $\bar{k}$) vary with depth only, specific heat capacity C_p is constant, $\Delta\rho_{thermal}$ is the fractional density variation with temperature ($=\alpha_{dimensional}\Delta T_{dimensional}$) and $\eta(C,z,T)$ is discussed later. z is the vertical coordinate (positive upwards). Viscosity η varies with temperature and depth, and often with strain rate, composition, and phase (e.g., Schubert, et al. [1];Tackley and Xie [2]).

Both 3-D (Cartesian) and 2-D (Cartesian, axisymmetric or cylindrical) domains are implemented. Top and bottom boundaries are impermeable, free-slip or rigid, and isothermal or insulating, while side boundaries are periodic or reflecting.

3. Numerical method

3.1. General

Variables are defined on a staggered grid (e.g., Patankar [3]). A global velocity/pressure solution is obtained at each time, with timestepping of T and C fields performed separately. The code is parallelized using MPI and run efficiently on parallel supercomputers and Beowulf clusters.

nodes	Grid	Time/V-cycle (s)	Efficiency (%)
1	32,32,32	2.68	100
2	64,32,32	2.77	97
4	64,64,32	2.92	92
8	64,64,64	2.95	91
16	128,64,64	2.97	90
32	128,128,64	3.18	84

Table 1

Performance of multigrid solver on a Beowulf cluster of 800 MHz Pentium 3 PCs with fast ethernet communication, using cell relaxation and a problem size scaled with #nodes.

Multigrid V-cycles are used for obtaining velocity/pressure solutions in an efficient manner (Table 1) but iterations may not converge when large viscosity gradients are present. The following strategies improve convergence, allowing viscosity to vary by a factor of several hundred between adjacent cells:

(i) Relaxing all variables in each cell (consisting of the central pressure and six surrounding velocity components) simultaneously, instead of one variable at a time (e.g., Patankar [3]). This is similar to the scheme of Vanka [4], except that the exact local inverse, rather than a diagonalized approximation, is used.

(ii) Careful restriction of the viscosity field to coarse grids using a modified version of the scheme by Trompert and Hansen [5].

(iii) Additional relaxations on coarse grids.

(iv) Additional relaxations in grid regions experiencing poor convergence. These regions are either detected automatically or specified in advance.

(v) Taking account of fine-grid viscosity variations in the coarse-to-fine (prolongation) operator.

The finite-volume method MPDATA by Smolarkiewicz [6] is used to advect the temperature field, while finite differences are used for the other terms in Eq 3. For the nondiffusive C field (Eq. 4), particles are used, as in Tackley and King [7] and Tackley [8].

3.2 Melting and differentiation

Partial melting in the shallow mantle supplies magma that may subsequently become crust. Because the composition of this magma is different from that of the unmelted material, this differentiates the mantle in major and trace elements.

Here, C represents the fraction of crustal material, varying from 0 (depleted) to 1 (pure crust). Melt is generated when the temperature exceeds a solidus based on experimental data (Herzberg, et al. [9]) and instantly erupts, forming crust. This vertical transfer of mass entails compaction of the melting region and downwards advection of overlying material, making room for the new crust on top, a process that is modeled as a separate step. Melting and eruption is discretized because composition is represented by particles.

Every particle tracks several trace elements. When partial melting occurs in a cell, concentrations are calculated by integrating over particles in that cell. The partitioning of trace elements between melt (new crust) and remaining solid is then calculated as in Christensen and Hofmann [10]. A specified fraction of erupting noble gases escapes to the atmosphere. Thus, trace element compositions of mantle materials can be compared to actual geochemical observations (summarized in Hofmann [11]).

3.3 Multiple phase transitions

The mixture of minerals in mantle rock depends on composition, pressure (depth) due to solid-solid phase transitions, and temperature due to their finite Clapeyron slopes.

#	Depth (km)	T (K)	□□ (kg/m^3)	□(MPa/K)
		Olivine system		
1	410	1600	280	+2.5
2	660	1900	400	-2.5
		Pyroxene-garnet system		
1	60	0	350	0
2	400	1600	150	+1.0
3	720	1900	500	+1.0

Table 2
Phase transition properties. □is the Clapeyron slope.

A simplified description is implemented based on mineral physics data (e.g., Irifune and Ringwood [12]; Ono, et al. [13]). Minerals are divided into the olivine system and the pyroxene-garnet (px-gt) system, which undergo different phase transitions (Table 2). Density vs. depth for these systems (Figure 1) shows a steady increase from adiabatic compression plus steps due to phase transitions. Phase transition depths depend on temperature according to the Clapeyron slopes (Figure 1 assumes an adiabat with 1600 K potential temperature).

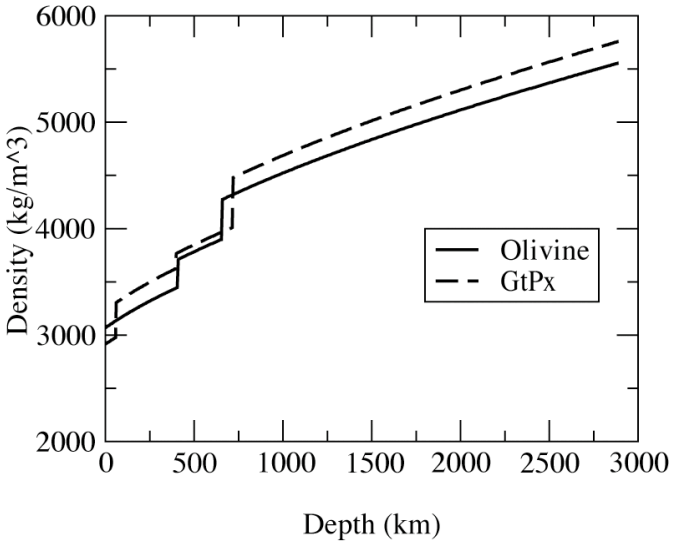

Figure 1. Density variation with depth along a reference adiabat for the two phase systems.

Density is calculated assuming that 'crust' (C=1) is pure px-gt while C=0 is 6:1 olivine:px-gt, and that the components can be added linearly:

$$\rho(C,z,T) = \left[\tfrac{6}{7}(1-C)\rho_{olivine}(z,T) + \tfrac{1}{7}(6C+1)\rho_{px-gt}(z,T)\right]\left[1-\alpha\left(T-\bar{T}(z)\right)\right]\rho_{thermal} \quad (5)$$

where the $\bar{\rho}(z,T)$ terms depend on depth and phase and the last term accounts for thermal expansion. $\bar{T}(z)$ is the reference adiabat (1600 K potential temperature).

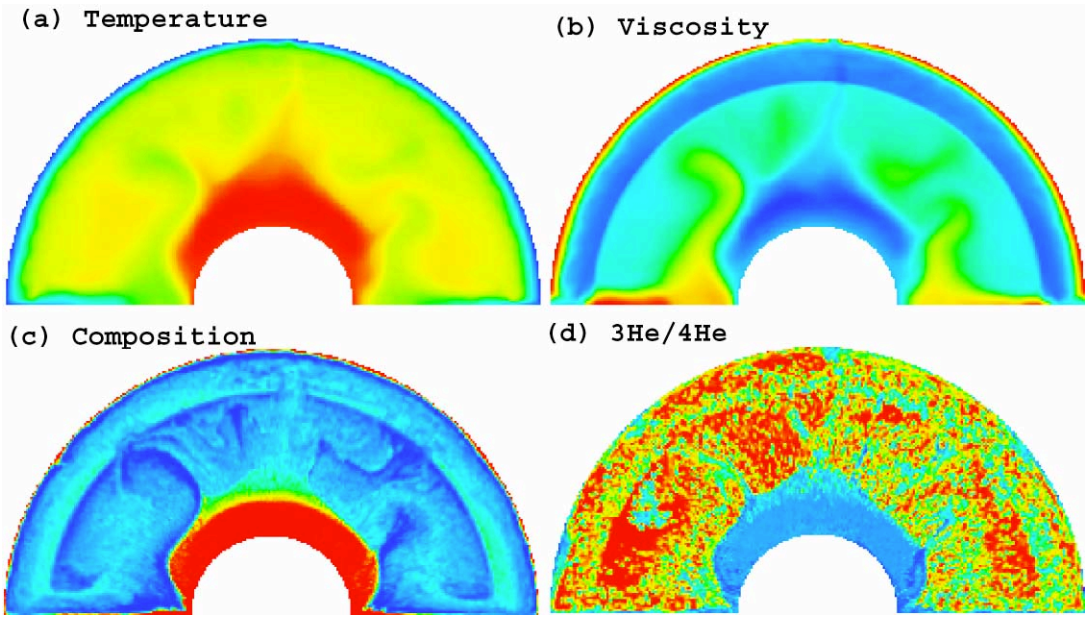

Figure 2. A sample result. (a) Temperature, from coldest (blue) to hottest (red), (b) log(viscosity), varying by factor 10^6, (c) composition, from crust (red) to depleted (blue), (d) ratio of ^{3}He/^{4}He, from 1.8 (blue) to 35 (red).

4. Sample results

An example simulation (Figure 2) from a homogeneous initial condition, similar to those in Tackley and Xie [2], displays several interesting features. The viscosity field indicates that the cold upper boundary layer is strong but develops weak zones that allow plate-like motion to occur. The composition field displays strong stratification due to the relative densities of the different components and their interaction with phase transitions: a layer of dense crust at the base, and a trapping of depleted material below 700 km depth. Helium ratios vary over the observed range.

5. Conclusion

Treatments of melting-induced compositional differentiation and multiple phase transitions have been successfully implemented in the code Stag3D, and are being used to improve our understanding of Earth's interior dynamics and evolution.

References

1. Schubert G, Turcotte DL, Olson P. Mantle Convection in the Earth and Planets. Cambridge University Press, 2000.
2. Tackley PJ, Xie S. The thermo-chemical structure and evolution of Earth's mantle: constraints and numerical models. Phil. Trans. R. Soc. Lond. A 2002;
3. Patankar SV. Numerical Heat Transfer and Fluid Flow. New York: Hemisphere Publishing Corporation, 1980.
4. Vanka SP. Block implicit multigrid solution of Navier-Stokes equations with primitive variables. J. Comp. Phys. 1986; 138-158.
5. Trompert RA, Hansen U. The application of a finite-volume multigrid method to 3-dimensional flow problems in a highly viscous fluid with a variable viscosity. Geophys. Astrophys. Fluid Dyn. 1996; 3-4:261-291.
6. Smolarkiewicz PK. A fully multidimensional positive definite advection transport algorithm with small implicit diffusion. J. Comp. Phys. 1984; 2:325-362.
7. Tackley PJ, King SD. Testing the tracer ratio method for modeling active compositional fields in mantle convection simulations. Geochem. Geophys. Geosyst. 2002; submitted.
8. Tackley PJ. Strong heterogeneity caused by deep mantle layering. Geochem. Geophys. Geosystems 2002; 4:10.1029/2001GC000167.
9. Herzberg C, Raterron P, Zhang J. New experimental observations on the anhydrous solidus for peridotite klb-1. Geochem. Geophys. Geosyst. 2000; 2000GC000089.
10. Christensen UR, Hofmann AW. Segregation of subducted oceanic crust In the convecting mantle. J. Geophys. Res. 1994; B10:19867-19884.
11. Hofmann AW. Mantle geochemistry: the message from oceanic volcanism. Nature 1997; 6613:219-29.
12. Irifune T, Ringwood AE. Phase-Transformations In Subducted Oceanic-Crust and Buoyancy Relationships At Depths Of 600-800 Km In the Mantle. Earth and Planetary Science Letters 1993; 1-2:101-110.
13. Ono S, Ito E, Katsura T. Mineralogy of subducted basaltic crust (MORB) from 25 to 37 GPa, and chemical heterogeneity of the lower mantle. Earth Planet. Sci. Lett. 2001; 1-2:57-63.